Reaction Kinetics

A Linear Free Energy Relationship for Gas-Solid Interactions: Correlation between Surface Rate Constant and Diffusion Coefficient of Oxygen Tracer Exchange for Electron-Rich Perovskites

Rotraut Merkle, Joachim Maier, and Henny J. M. Bouwmeester*

Reactivity and transport properties can be traced back to materials parameters and control parameters. As far as the concentrations of electronic and ionic charge carriers are concerned, partial pressures P of the components, temperature T, and dopant content C are the most important control parameters. While their influence is often well-understood on a phenomenological level, the understanding of materials parameters such as enthalpies and entropies of reaction or activation usually requires an atomistic analysis. Phenomenological relationships connecting these parameters are very rare and, if established, extremely useful. The most prominent examples stem from organic solution chemistry, for example, the effect of substrate substitution on aromatic reactions (cf. the Hammett equation) or the Brönsted catalysis relation.[1] These equations make use of a linear correlation between free activation enthalpy and free reaction enthalpy. Specifically, when enthalpies instead of free enthalpies are considered, this may be termed an Evans–Polanyi relationship.[2] A few attempts to verify linear (free) energy relationships in solid-state chemistry have been reported,[3] but without deeper insight into the mechanistic details or a conclusive correlation between data and model. Here we unambiguously demonstrate the validity of such a linear (free) energy relationship for inorganic solid-state reactions.

The interaction of gaseous O_2 with oxides is of technical relevance as well as of fundamental interest, and tracer experiments are an important tool for its investigation. The oxygen incorporation comprises the surface reaction from O_2 to oxide ions in the first bulk layer, and subsequent diffusion of oxide ions within the bulk. A surprising and strongly debated relationship between the experimentally determined effective surface rate constant $\bar{k}^*$ and oxygen tracer diffusion coefficient D^* was found for the family of $(La_{1-x}Sr_x)(Mn_{1-y}Co_y)O_{3-z}$, $(La_{1-x}Sr_x)(Fe_{1-y}Co_y)O_{3-z}$, and $(Sm_{1-x}Sr_x)CoO_{3-z}$

[*] Dr. R. Merkle, Prof. Dr. J. Maier
Max-Planck-Institut für Festkörperforschung
Heisenbergstrasse 1
70569 Stuttgart (Germany)
Fax: (+49) 711-689-1722
E-mail: sofia.weiglein@fkf.mpg.de
Prof. Dr. H. J. M. Bouwmeester
Department of Science and Technology &
MESA+ Research Institute for Nanomaterials
University of Twente (The Netherlands)

Supporting information for this article (containing details of the kinetic treatment: derivation of Eqs. (9) and (12) and discussion of alternative mechanisms) is available on the WWW under http://www.angewandte.org or from the author.

 DOI: 10.1002/ange.200460081

perovskites (Figure 1).[4,5] To a good approximation, both quantities were reported to be related by the power law given in Equation (1). Assuming Arrhenius-type expressions for $\bar{k}^*$

$$\log \bar{k}^* \cong a + b \log D^* \quad (a \cong -1,\ b \cong 0.5) \tag{1}$$

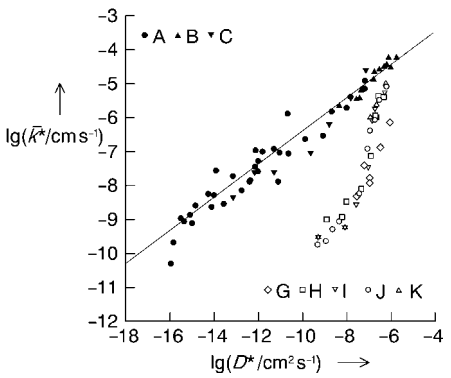

Figure 1. Correlation of the effective surface rate constant $\bar{k}^*$ with the oxygen tracer diffusion coefficient D^*, reprinted from ref. [5] with permission from Elsevier, copyright 1999. A = $(La,Sr)(Mn,Co)O_{3-z}$, B = $(Sm,Sr)(Co)O_{3-z}$, C = $(La,Sr)(Co,Fe)O_{3-z}$ (electron-rich transition metal perovskites); G = $La_{0.9}Sr_{0.1}Ga_{0.8}Mg_{0.2}O_{2.85}$, H = $Zr_{0.85}Y_{0.15}O_{1.925}$, I = $Ce_{0.90}Gd_{0.1}O_{1.95}$, J = $Zr_{0.81}Y_{0.19}O_{1.905}$ single crystal, K = $Ce_{0.69}Gd_{0.31}O_{1.845}$ single crystal (electron-poor electrolyte materials). The line represents the $\bar{k}^*$–D^* correlation for samples A–C, as discussed in the text, and has a slope of $b = 0.5$.

and D^*, this implies an interrelation of the effective activation energies as well as the prefactors [Eqs. (2), (3)].

$$E_{k*} = b\, E_{D*} \tag{2}$$

$$\log k_0^* = a + b \log D_0^* \tag{3}$$

The data points in Figure 1 comprise variations in temperature, oxygen partial pressure, and composition of the perovskite phase. What makes Equation (1) so interesting and simultaneously so hard to understand is that its range of validity covers all materials within a given class and hence implies a variation of materials parameters such as reaction enthalpies. Figure 1 also shows data for electron-poor electrolyte materials (G–K): They deviate strongly from the line discussed below, indicating that these correlations hold only for families of materials with similar mechanistic parameters.

A detailed treatment of effective rate constants has previously been given that showed how $\bar{k}^{\varepsilon}$ ($\varepsilon = *$ (tracer), δ (chemical experiment), Q (electrical experiment)) can be obtained as a function of the control parameters P, C, and T.[6] The temperature is essentially introduced through the microscopic rate constant of the rate determining step (rds) and through the mass action constants K_q of the fast reactions that have to be coupled in the kinetic scheme. Close to equilibrium and for a given parameter window, $\bar{k}^*$ is given by Equation (4); $\mathring{A}_0^*$ is the equilibrium exchange rate, $\langle k \rangle$ denotes the geometric means of the forward and backward rate constants (subscript s indicates "surface"). The expression for D^* is,

$$\bar{k}^* \propto \mathring{A}_0^*(\mathrm{rds}) = \langle k \rangle_{\mathrm{rds}}(T) \sum_q K_q^{\gamma_s}(T)\, C^{M_s}\, P^{N_s} \tag{4}$$

under Brouwer and Boltzmann conditions, determined with Equation (5), with σ and u being the conductivity and mobility of the mobile defect (the subscript ∞ refers to "bulk").

$$D^* \propto \sigma_\infty = u(T) \sum_r K_r^{\gamma_\infty}(T)\, C^{M_\infty}\, P^{N_\infty} \tag{5}$$

For a given mechanistic scheme, these equations allow one to derive directly $\bar{k}^*$ versus D^* upon variation of p, C, or T. For a given material, a linear $\log \bar{k}^* - \log D^*$ relationship follows automatically if Arrhenius-type expressions hold for $\bar{k}^*$ and D^* individually. If, however, the material is varied, as is the case here, the question becomes more delicate because then the enthalpy and entropy parameters in the above equations become variables themselves. A linear relationship as given in references [4,5] (see Figure 1) betrays the validity of further more subtle features of the materials. Since the mapping of $D^* \leftrightarrow \bar{k}^*$ involves various mass action "constants" and kinetic "constants", a family relationship between reaction free enthalpies and activation free enthalpies may be anticipated.

Here we will show that the relationship given in Equation (6) correctly explains Figure 1 (δ denotes the compositional variation within the materials family). We also demonstrate that Equation (6) can be mechanistically corroborated and even tested by independent results. Since the entropies are mostly structurally determined and do not significantly change from material to material within the family under consideration, Equation (6) also represents a free energy relationship (owing to the small and constant mechanical work term, we do not differentiate between energy and enthalpy).

$$\delta \Delta H_{\mathrm{rds}}^{\ddagger} = -0.5\, \delta \Delta H_{\mathrm{ox}}^0 \tag{6}$$

The tracer diffusion in the bulk follows a vacancy mechanism [Eq. (7), f = correlation factor = 0.69[4]], where

$$D^* = f \frac{[V_O^{\cdot\cdot}]}{c_O} D_{V_O^{\cdot\cdot}} = 0.69 \frac{[V_O^{\cdot\cdot}]}{c_O} D_{V_O^{\cdot\cdot}}\, e^{-\Delta H_V^{\ddagger}/k_B T} \tag{7}$$

the vacancy jump activation enthalpy $H_V^{\ddagger}$ of about 0.9 eV (= oxide ion jump activation enthalpy) and the prefactor D_O are approximately constant for all the samples within the materials family considered.[7,8,4] The material- and temperature-dependent vacancy concentration $[V_O^{\cdot\cdot}]$ can be calculated from the overall oxygen incorporation reaction [Eq. (8)]

$$\frac{1}{2} O_2 + V_O^{\cdot\cdot} \rightleftharpoons O_O^{\times} + 2\,h^{\cdot} \tag{8}$$

with a reaction enthalpy ΔH_{ox}^0 that is typically negative. Insertion of the mass action constant corresponding to the reaction in Equation (8) into Equation (7) shows that the overall D^* activation enthalpy includes contributions from vacancy formation and migration [Eq. (9), see the Supporting Information for details].

$$E_{D*} = -\Delta H_0^{ox} + \Delta H_V^{\ddagger} \quad (9)$$

Now let us select a reasonable mechanism for the surface reaction that operates for all the materials considered (it will be outlined later that within certain limits the details of the mechanism do not affect the validity of this rationale). Whereas for electron-poor materials the electron-transfer steps might be crucial for the overall rate, this is not likely to be the case for the electron-rich materials under regard. (The term "electron-rich" refers to the presence of excess electrons or to the presence of regular, but easily transferable electrons, and hence also includes the p-type conductors.[9]) Although no direct evidence for the presence of adsorbed atomic oxygen species such as O^- exists for the materials considered here (largely due to experimental limitations), desorption measurements indicate their formation above 400 °C.[10] On ZnO and SnO_2 the ratio of O^- to O_2^- increases with increasing temperature.[11] Oxygen permeation measurements under surface limited conditions yield a reaction order of $\frac{1}{2}$ for O_2 (see e.g. $SrCo_{0.8}Fe_{0.2}O_{3-z}$[12] and $La_{0.5}Sr_{0.5}Ga_{0.2}Fe_{0.8}O_{3-z}$[13]), which indicates that only atomic oxygen species are involved in the rate determining step. The relationship in Equation (2) between the effective activation energies of $\bar{k}^*$ and D^* and the mechanism of the diffusion process resulting in Equation (9) imply a significant contribution $b\,\Delta H_V^{\ddagger}$ to the effective activation energy E_{k^*} of the surface reaction, which stems from the $V_O^{\cdot\cdot}$ jump activation enthalpy. This may be seen as an indication that a $V_O^{\cdot\cdot}$ site exchange is involved in the rds, as already qualitatively concluded in ref. [5].

Hence, we assume that the reaction rate is determined by the ion transfer step, that is, by the incorporation of ionized atomic oxygen into the vacancy. The degree of ionization of surface oxygen is definitely less than two but more than zero, so that we adopt the mechanism given by Equations (10) and (11) (Kröger–Vink nomenclature, see the Supporting Information for other mechanisms). The resulting tracer exchange

$$\frac{1}{2}O_2 \rightleftharpoons O' + h^{\cdot} \quad \text{pre-equilibrium} \quad (10)$$

$$O' + V_O^{\cdot\cdot} \rightleftharpoons O_O^x + h^{\cdot} \quad \text{rate-determining step (rds)} \quad (11)$$

rate is given by Equation (12) (see reference [6] for the

$$\bar{k}^* = \frac{1}{c_O}\sqrt{\overrightarrow{k}\,\overleftarrow{k}\,[O'][V_O^{\cdot\cdot}][h^{\cdot}]} = \left(\frac{\overrightarrow{k}_0[h^{\cdot}]}{c_O}\right) e^{-\Delta \overleftarrow{H}^*/k_B T} \quad (12)$$

method of derivation and the Supporting Information for details; all concentrations refer to equilibrium, c_O = oxide ion concentration ≈ constant, $\overrightarrow{k}$ and $\overleftarrow{k}$ denote the forward and backward rate constants and may also include built-in electrical fields). The overall activation enthalpy approximately equals the activation enthalpy $\overleftarrow{H}^{\ddagger}$ of the backward reaction in reaction (11) [Eq. (13)].

$$E_{k*} \approx \Delta \overleftarrow{H}^{\ddagger} \quad (13)$$

As all data are measured in a limited pO_2 range (typically 10^{-3} bar $\le pO_2 \le 1$ bar), the variation of $\bar{k}^*$ and D^* with pO_2 can be neglected (typically $\bar{k}^*$, $D^* \propto (pO_2)^n$ where $|n| \le 0.5$). Consequently, we are left with variations of temperature and sample composition. For Equation (1) to hold, the effective activation energies must fulfil the condition resulting from inserting Equations (9) and (13) into Equation (2) with $b \cong 0.5$ [Eq. (14), see the Supporting Information for the treatment of the prefactors k_0^*, D_0^*].

$$\Delta \overleftarrow{H}^{\ddagger} = b\,(\Delta H_V^{\ddagger} - \Delta H_{ox}^0) = 0.45\,\text{eV} - 0.5\,\Delta H_{ox}^0 \quad (14)$$

This is indeed a linear relationship between an activation enthalpy and a reaction enthalpy. The importance of Equation (14) lies in the fact that $\delta\Delta \overleftarrow{H}^{\ddagger} = -0.5\,\delta\Delta H_{ox}^0$, that is, the slope (0.5) and the intercept (0.45 eV) do not perceptibly change when the material is varied within the family under concern. According to Equation (13), $\Delta \overleftarrow{H}^{\ddagger}$ is approximately identical to the effective activation energy of $\bar{k}^*$, and we arrive at the experimentally testable prediction that E_{k^*} varies linearly with the overall oxygen incorporation enthalpy ΔH_{ox}^0 when the sample composition varies. Figure 2 displays this

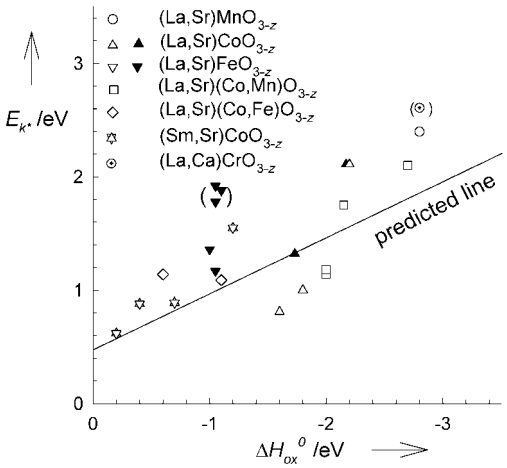

Figure 2. Correlation of the experimentally determined activation energy of surface exchange E_{k^*} and the overall oxygen incorporation enthalpy ΔH_{ox}^0. Closed symbols: experimental ΔH_{ox}^0 data available, open symbols: ΔH_{ox}^0 estimated either from experimental D^* data and $\Delta H_V^{\ddagger} = 0.9$ eV [see Eq. (9)] or from experimental data for materials with a slightly different composition. The line represents the predicted linear free energy relationship [Eq. (14)]. The data are from references [4, 5, 16] as well as [7, 17] ($(La,Sr)CoO_{3-z}$), [7, 18] ($(La,Sr)FeO_{3-z}$), [19] ($(La,Sr)(Co,Fe)O_{3-z}$), and [20, 21] ($(La,Ca)CrO_{3-z}$

correlation (and includes materials of the same family that are not contained in Figure 1). The experimental E_{k^*} data tend to be slightly above the line predicted from Equation (14), which might be due to the small temperature dependence of the electronic charge carriers [see Eq. (12)]. Keeping in mind the experimental uncertainties (the typical error of E_{k^*} is 0.2 eV;[5] for $(La,Ca)FeO_{3-z}$ the data points in parentheses stem from similar sample compositions, but were measured by a different group[7] as well as the approximations made in deriving Equation (14), the agreement is satisfactory (the deviation of $(La,Ca)CrO_{3-z}$ might be due to the comparably strong d electron localization[14]).

The main point is now the interpretation of Equation (14) on a mechanistic level. First, we have to emphasize again that such a relationship can only be valid for a class of materials for which the same mechanism is operative. The contributions of $\Delta H_V^{\ddagger}$ and ΔH_{ox}^0 to $\Delta \overleftarrow{H}^{\ddagger}$ can be rationalized as follows: After the fast preequilibrium reaction (10), the activation energy of the rds has to be overcome (Figure 3); the rds is the transfer of

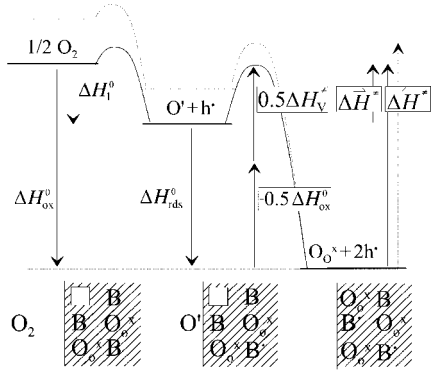

Figure 3. Top: Enthalpy diagram of oxygen incorporation according to reactions (10) and (11). The decomposition of $\Delta \overleftarrow{H}^{\ddagger}$ into contributions from $\Delta H_V^{\ddagger}$ and ΔH_{ox}^0 is based on Equation (14). The dashed lines indicate the variation of the material, which results in a coupled increase of ΔH_{ox}^0 and $\Delta \overleftarrow{H}^{\ddagger}$ (for clarity the enthalpy profiles are normalized such that the final state exhibits the same energy level for both cases). Bottom: mechanistic picture of the reaction.

adsorbed O′ into a vacancy with the simultaneous oxidation of the valence band ion (the B cation in Figure 3). Since the transferred atomic oxygen species is not a fully charged oxide ion, but has a charge between -1 and -2 (being approximately constant among the materials considered), and since the transfer occurs between the surface and the first bulk layer, we can assume that the threshold is reduced compared to bulk diffusion. Therefore, the contribution of the ionic motion to the overall activation enthalpy $\Delta \overleftarrow{H}^{\ddagger}$ is not $\Delta H_V^{\ddagger}$, but only a constant fraction $b\,\Delta H_V^{\ddagger}$. The actual numerical value $b \cong 0.5$ as given by the experimentally observed correlation is consistent with this picture. When passing through the rds, the reaction enthalpy of this step, ΔH_{rds}^0, is released, and a fraction γ of it (the exact value depends on the precise location of the transition state on the reaction coordinate) is involved in the activation process (i.e., up to the transition state) and contributes to $\Delta \overleftarrow{H}^{\ddagger}$. Since for ΔH_{rds}^0 it can be estimated that $|\Delta H_{rds}^0| \leq |\Delta H_{ox}^0|$, the experimentally observed contribution of $-0.5\,\Delta H_{ox}^0$ to $\Delta \overleftarrow{H}^{\ddagger}$ [Eq. (14)] implies a value of $\gamma \geq 0.5$ and thus a transition state closer to the intermediate state O′ than to the final state O_O^x. The numerical prefactors that account for the $\Delta H_V^{\ddagger}$ and the ΔH_{ox}^0 contributions to $\Delta \overleftarrow{H}^{\ddagger}$ are probably not completely identical, but the experimentally observed $\bar{k}^*-D^*$ correlation shows that $b \cong 0.5$ is indeed a good approximation.

Assuming as a first approximation that the oxygen site exchange is not influenced by the variation in composition (as supported by the observed constancy of $\Delta H_V^{\ddagger}$), the variation of $\Delta \overleftarrow{H}^{\ddagger}$ with composition refers to the partial electron transfer from the B cation to the oxygen in the transition state (the degree of intermediate charge is roughly independent of sample composition).[15] Finally, the constancy of the parameter b reflects the validity of the same mechanism for all materials considered as well as the chemical and structural similarity of the family members. An important feature of the analysis is that the activation energy of vacancy migration also contributes to the surface reaction, which is attributed to the fact that the latter involves not only an electron transfer but also represents an ion site exchange. In the Supporting Information, two other hypothetical mechanisms are discussed which fulfil the prerequisites (atomic oxygen species as well as $V_O^{\cdot}$ in the rds). While one of these mechanisms is rather improbable, the other leads to similar conclusions. This demonstrates the validity of the given arguments irrespective of minor mechanistic details.

To summarize, we have shown that the astonishing $\bar{k}^*-D^*$ correlation for electron-rich perovskites can be understood on the basis of a linear free enthalpy relationship for gas–solid reactions. This relationship assumes a constant coupling between the $\bar{k}^*$ activation enthalpy and the oxidation reaction enthalpy (constant with regard to variation among the materials family considered). This point was independently tested by referring to kinetic and themodynamic data from the literature. The treatment demonstrates the usefulness of linear free energy relationships, which are state of the art for organic solution chemistry, for inorganic solid-state reactions.

Received: January 23, 2004
Revised: June 21, 2004

Keywords: charge transfer · defect chemistry · diffusion · kinetics · oxygen exchange

[1] See textbooks of organic chemistry, for example, J. March, *Advanced Organic Chemistry*, Wiley, New York, **1992**, p. 258 and p. 278.
[2] See, for example, B. P. Roberts, A. J. Steel, *J. Chem. Soc. Perkin Trans. 2* **1994**, 2155–2162.
[3] a) R. Kapoor, S. T. Oyama, *J. Mater. Res.* **1997**, *12*, 474–479; b) D. A. Sverjensky, *Nature* **1992**, *358*, 310–313.
[4] J. A. Kilner, R. A. De Souza, I. C. Fullarton, *Solid State Ionics* **1996**, *86*, 703–709.
[5] R. A. De Souza, J. Kilner, *Solid State Ionics* **1999**, *126*, 153–161.
[6] a) J. Maier, *Solid State Ionics* **1998**, *112*, 197–228; b) J. Maier, *Solid State Ionics* **2000**, *135*, 575–588.
[7] T. Ishigaki, S. Yamauchi, K. Kishio, J. Mizusaki, K. Fueki, *J. Solid State Chem.* **1988**, *73*, 179–187.
[8] J. Mizusaki, I. Yasuda, J. Shimoya, S. Yamauchi, F. Fueki, *J. Electrochem. Soc.* **1993**, *140*, 467–471.
[9] T. Ohtani, K. Kuroda, K. Matsugami, D. Katoh, *J. Eur. Ceram. Soc.* **2000**, *20*, 2721–2726.
[10] S. C. Chang, *J. Vac. Sci. Technol.* **1980**, *17* 366–369.
[11] M. Iwamoto, Y. Yoda, N. Yamazoe, T. Selyama, *J. Phys. Chem.* **1978**, *82*, 2564–2570.
[12] H. J. M. Bouwmeester, H. Kruidhof, A. J. Burggraf, *Solid State Ionics* **1994**, *72*, 185–194.
[13] S. Kim, S. Wang, X. Chen, Y. L. Wang, N. Wu, A. Ignatiev, A. J. Jacobson, B. Abeles, *J. Electrochem. Soc.* **2001**, *147*, 2398–2406.

[14] D. P. Karim, A. T. Aldred, *Phys. Rev. B* **1979**, *20*, 2255 – 2263.
[15] This fractional change in the rds activation energy with variation in the reagent–product energy difference bears some reminiscence to the Butler–Volmer equation even though the latter only makes a statement on the electrical field distribution.
[16] R. A. De Souza, J. A. Kilner, *Solid State Ionics* **1998**, *106*, 175 – 187.
[17] a) J. Mizusaki, Y. Mima, S. Yamauchi, K. Fueki, H. Tagawa, *J. Solid State Chem.* **1989**, *80*, 102 – 111; b) M. H. R. Lankhorst, H. J. M. Bouwmeester, H. Verweij, *J. Solid State Chem.* **1997**, *133*, 555 – 567; c) T. Ishigaki, S. Yamauchi, J. Mizusaki, K. Fueki, H, Tamura, *J. Solid State Chem.* **1984**, *54*, 100 – 107.
[18] a) J. Mizusaki, M. Yoshihiro, S. Yamauchi, K. Fueki, *J. Solid State Chem.* **1985**, *58*, 257 – 266; b) J. E. ten Elshof, M. H. R. Lankhorst, H. J. M. Bouwmeester, *J. Electrochem. Soc.* **1997**, *144*, 1060 – 1066.
[19] a) J. A. Lane, S. J. Benson, D. Waller, J. A. Kilner, *Solid State Ionics* **1999**, *121*, 201 – 208; b) S. Carter, A. Selcuk, R. J. Chater, J. Kajda, J. A. Kilner, B. C. H. Steele, *Solid State Ionics* **1992**, *53*, 597 – 605.
[20] J. Mizusaki, S. Yamauchi, K. Fueki, A. Ishikawa, *Solid State Ionics* **1984**, *12*, 119 – 124.
[21] I. Yasuda, K. Ogasawara, M. Hishinuma, *J. Am. Ceram. Soc.* **1997**, *80*, 3009 – 3012.

